# 4-Gbit/s visible light communication link based on 16-QAM OFDM transmission over remote phosphor-film converted white light by using blue laser diode

**José Ramón Durán Retamal,[1] Hassan Makine Oubei,[1] Bilal Janjua,[1] Yu-Chieh Chi,[2] Huai-Yung Wang,[2] Cheng-Ting Tsai,[2] Tien Khee Ng,[1] Dan-Hua Hsieh,[3] Hao-Chung Kuo,[3] Mohamed-Slim Alouini,[1] Jr-Hau He,[1,4] Gong-Ru Lin,[2,5] and Boon S. Ooi[1,6]**

[1]*Computer, Electrical and Mathematical Sciences and Engineering Division, King Abdullah University of Science and Technology, Thuwal 23955-6900, Saudi Arabia*

[2]*Graduate Institute of Photonics and Optoelectronics, and Department of Electrical Engineering, National Taiwan University, 1, Roosevelt Road Section 4, Taipei 10617, Taiwan*

[3]*Department of Photonics and Institute of Electro-Optical Engineering, National Chiao-Tung University, 1001 Ta Hsueh Road, Hsinchu 30013, Taiwan*

[4]*jrhau.he@kaust.edu.sa*

[5]*grlin@ntu.edu.tw*

[6]*boon.ooi@kaust.edu.sa*

**Abstract:** Visible Light Communication (VLC) as a new technology for ultrahigh-speed communication is still limited when using slow modulation light-emitting diode (LED). Alternatively, we present a 4-Gbit/s VLC system using coherent blue-laser diode (LD) *via* 16-quadrature amplitude modulation orthogonal frequency division multiplexing. By changing the composition and the optical-configuration of a remote phosphor-film the generated white light is tuned from cool day to neutral, and the bit error rate is optimized from $1.9 \times 10^{-2}$ to $2.8 \times 10^{-5}$ in a blue filter-free link due to enhanced blue light transmission in forward direction. Briefly, blue-LD is an alternative to LED for generating white light and boosting the data rate of VLC.



**OCIS codes:** (060.4510) Optical communications; (060.4250) Networks; (140.2020) Diode lasers; (060.2630) Frequency modulation; (060.2605) Free-space optical communication.

## References and links

1. M. O'Grady and G. O'Hare, "Computer science. How smart is your city?" Science **335**(6076), 1581–1582 (2012).
2. R. Won, "View from... communication networks beyond the capacity crunch: Is it crunch time?" Nat. Photonics **9**(7), 424–426 (2015).
3. M. Jinno, Y. Miyamoto, and Y. Hibino, "Networks: optical-transport networks in 2015," Nat. Photonics **1**(3), 157–159 (2007).
4. News, "Wireless future drives microwave photonics," Nat. Photonics **5**(12), 724 (2011).
5. H. Elgala, R. Mesleh, and H. Haas, "Indoor optical wireless communication: potential and state-of-the-art," IEEE Commun. Mag. **49**(9), 56–62 (2011).
6. W. Ding, F. Yang, H. Yang, J. Wang, X. Wang, X. Zhang, and J. Song, "A hybrid power line and visible light communication system for indoor hospital applications," Comput. Ind. **68**, 170–178 (2015).
7. R. Perez-Jimenez, J. Rufo, C. Quintana, J. Rabadan, and F. J. Lopez-Hernandez, "Visible light communication systems for passenger in-flight data networking," in *IEEE International Conference on Consumer Electronics (*ICCE, 2011), pp. 445–446.
8. N. Kumar, N. Lourenco, D. Terra, L. N. Alves, and R. L. Aguiar, "Visible light communications in intelligent transportation systems," in *IEEE Intelligent Vehicles Symposium (*IV, 2012), pp. 748–753.
9. I. Takai, T. Harada, M. Andoh, K. Yasutomi, K. Kagawa, and S. Kawahito, "Optical vehicle-to-vehicle communication system using LED transmitter and camera receiver," IEEE Photonics J. **6**(5), 1–14 (2014).
10. T. Yamazato, I. Takai, H. Okada, T. Fujii, T. Yendo, S. Arai, M. Andoh, T. Harada, K. Yasutomi, K. Kagawa, and S. Kawahito, "Image-sensor-based visible light communication for automotive applications," IEEE Commun. Mag. **52**(7), 88–97 (2014).

#251468 Received 9 Oct 2015; revised 9 Dec 2015; accepted 15 Dec 2015; published 21 Dec 2015

11. G.-y. Hu, C.-y. Chen, and Z. Chen, "Free-space optical communication using visible light," J. Zhejiang University **8**(2), 186–191 (2007).
12. T. Morio, T. Hideki, K. Yoshisada, T. Yoshihisa, K. Hiroo, K. Toshihiro, S. Kenji, Y. Shinich, T. Shinich, T. Hiroyuki, N. Isao, and A. Maki, "Terrestrial free-space optical communications network for future airborne and satellite-based optical communications projects," in *31st AIAA International Communications Satellite Systems Conference* (ICSSC, 2013).
13. D. Iturralde, C. Azurdia-Meza, N. Krommenacker, I. Soto, Z. Ghassemlooy, and N. Becerra, "A new location system for an underground mining environment using visible light communications," in *9th International Symposium on Communication Systems, Networks & Digital Signal Processing* (CSNDSP, 2014), pp. 1165–1169.
14. H. M. Oubei, J. R. Duran, B. Janjua, H.-Y. Wang, C.-T. Tsai, Y.-C. Chi, T. K. Ng, H.-C. Kuo, J.-H. He, M.-S. Alouini, G.-R. Lin, and B. S. Ooi, "4.8 Gbit/s 16-QAM-OFDM transmission based on compact 450-nm laser for underwater wireless optical communication," Opt. Express **23**(18), 23302–23309 (2015).
15. H. M. Oubei, C. Li, K.-H. Park, T. K. Ng, M.-S. Alouini, and B. S. Ooi, "2.3 Gbit/s underwater wireless optical communications using directly modulated 520 nm laser diode," Opt. Express **23**(16), 20743–20748 (2015).
16. P. Pust, P. J. Schmidt, and W. Schnick, "A revolution in lighting," Nat. Mater. **14**(5), 454–458 (2015).
17. D. O'Brien, H. Le Minh, L. Zeng, G. Faulkner, K. Lee, D. Jung, Y. Oh, and E. T. Won, "Indoor visible light communications: challenges and prospects," Proc. SPIE **7091**, 709106 (2008).
18. D. D. G. C. Jones, "Semiconductor devices for high-speed optoelectronics, by Giovanni Ghione," Contemp. Phys. **52**(2), 169–170 (2011).
19. A. M. Khalid, G. Cossu, R. Corsini, P. Choudhury, and E. Ciaramella, "1-Gb/s Transmission over a phosphorescent white LED by using rate-adaptive discrete multitone modulation," IEEE Photonics J. **4**(5), 1465–1473 (2012).
20. H. Li, X. Chen, J. Guo, and H. Chen, "A 550 Mbit/s real-time visible light communication system based on phosphorescent white light LED for practical high-speed low-complexity application," Opt. Express **22**(22), 27203–27213 (2014).
21. C. H. Yeh, C. W. Chow, H. Y. Chen, J. Chen, and Y. L. Liu, "Adaptive 84.44-190 Mbit/s phosphor-LED wireless communication utilizing no blue filter at practical transmission distance," Opt. Express **22**(8), 9783–9788 (2014).
22. C.-Y. Lin, Y.-P. Lin, H.-H. Lu, C.-Y. Chen, T.-W. Jhang, and M.-C. Chen, "Optical free-space wavelength-division-multiplexing transport system," Opt. Lett. **39**(2), 315–318 (2014).
23. J. Tan, K. Yang, and M. Xia, "Adaptive equalization for high speed optical MIMO wireless communications using white LED," Front. Optoelectron. China **4**(4), 454–461 (2011).
24. D. Tsonev, H. Chun, S. Rajbhandari, J. J. D. McKendry, S. Videv, E. Gu, M. Haji, S. Watson, A. E. Kelly, G. Faulkner, M. D. Dawson, H. Haas, and D. O'Brien, "A 3-Gb/s single-LED OFDM-based wireless VLC link using a gallium nitride μLED," IEEE Photonics Technol. Lett. **26**(7), 637–640 (2014).
25. F. M. Wu, C. T. Lin, C. C. Wei, C. W. Chen, Z. Y. Chen, H. T. Huang, and C. Sien, "Performance comparison of OFDM signal and CAP signal over high capacity RGB-LED-based WDM visible light communication," IEEE Photonics J. **5**(4), 7901507 (2013).
26. Y. Pei, S. Zhu, H. Yang, L. Zhao, X. Yi, J. J. Wang, and J. Li, "LED modulation characteristics in a visible-light communication system," Opt. Photonics J. **3**(2), 4 (2013).
27. J. J. Wierer, Jr., J. Y. Tsao, and D. S. Sizov, "Comparison between blue lasers and light-emitting diodes for future solid-state lighting," Laser Photonics Rev. **7**(6), 963–993 (2013).
28. S. Watson, M. Tan, S. P. Najda, P. Perlin, M. Leszczynski, G. Targowski, S. Grzanka, and A. E. Kelly, "Visible light communications using a directly modulated 422 nm GaN laser diode," Opt. Lett. **38**(19), 3792–3794 (2013).
29. Y.-C. Chi, D.-H. Hsieh, C.-T. Tsai, H.-Y. Chen, H.-C. Kuo, and G.-R. Lin, "450-nm GaN laser diode enables high-speed visible light communication with 9-Gbps QAM-OFDM," Opt. Express **23**(10), 13051–13059 (2015).
30. A. Neumann, J. J. Wierer, Jr., W. Davis, Y. Ohno, S. R. J. Brueck, and J. Y. Tsao, "Four-color laser white illuminant demonstrating high color-rendering quality," Opt. Express **19**(S4), A982–A990 (2011).
31. D. Tsonev, S. Videv, and H. Haas, "Towards a 100 Gb/s visible light wireless access network," Opt. Express **23**(2), 1627–1637 (2015).
32. B. Janjua, H. M. Oubei, J. R. D. Retamal, T. K. Ng, C.-T. Tsai, H.-Y. Wang, Y.-C. Chi, H.-C. Kuo, G.-R. Lin, J.-H. He, and B. S. Ooi, "Going beyond 4 Gbps data rate by employing RGB laser diodes for visible light communication," Opt. Express **23**(14), 18746–18753 (2015).
33. A. T. Hussein and J. M. H. Elmirghani, "Mobile multi-gigabit visible light communication system in realistic indoor environment," J. Lightwave Technol. **33**(15), 3293–3307 (2015).
34. H.-C. Kuo, C.-W. Hung, H.-C. Chen, K.-J. Chen, C.-H. Wang, C.-W. Sher, C.-C. Yeh, C.-C. Lin, C.-H. Chen, and Y.-J. Cheng, "Patterned structure of remote phosphor for phosphor-converted white LEDs," Opt. Express **19**(S4), A930–A936 (2011).
35. C.-Y. Chen, P.-Y. Wu, H.-H. Lu, Y.-P. Lin, J.-Y. Wen, and F.-C. Hu, "Bidirectional 16-QAM OFDM in-building network over SMF and free-space VLC transport," Opt. Lett. **38**(13), 2345–2347 (2013).
36. C. H. Yeh, H. Y. Chen, Y. L. Liu, and C. W. Chow, "Polarization-multiplexed 2×2 phosphor-LED wireless light communication without using analog equalization and optical blue filter," Opt. Commun. **334**, 8–11 (2015).
37. Y. Wang, C. Yang, Y. Wang, and N. Chi, "Gigabit polarization division multiplexing in visible light communication," Opt. Lett. **39**(7), 1823–1826 (2014).
38. J.-Y. Sung, C.-W. Chow, and C.-H. Yeh, "Is blue optical filter necessary in high speed phosphor-based white light LED visible light communications?" Opt. Express **22**(17), 20646–20651 (2014).

#251468 Received 9 Oct 2015; revised 9 Dec 2015; accepted 15 Dec 2015; published 21 Dec 2015

39. C. H. Yeh, C. W. Chow, H. Y. Chen, J. Chen, Y. L. Liu, and Y. F. Wu, "High-speed phosphor-LED wireless communication system utilizing no blue filter," Proc. SPIE **9193**, 91931A (2014).
40. J. Armstrong, "OFDM for optical communications," J. Lightwave Technol. **27**(3), 189–204 (2009).
41. R. Schmogrow, B. Nebendahl, M. Winter, A. Josten, D. Hillerkuss, S. Koenig, J. Meyer, M. Dreschmann, M. Huebner, C. Koos, J. Becker, W. Freude, and J. Leuthold, "Error vector magnitude as a performance measure for advanced modulation formats," IEEE Photonics Technol. Lett. **24**(1), 61–63 (2012).
42. A. C. C. Esteves, J. Brokken-Zijp, J. Laven, and G. de With, "Light converter coatings from cross-linked PDMS/particles composite materials," Prog. Org. Coat. **68**(1-2), 12–18 (2010).
43. R. A. Shafik, S. Rahman, and R. Islam, "On the extended relationships among EVM, BER and SNR as performance metrics," in *International Conference on Electrical and Computer Engineering* (ICECE, 2006), pp. 408–411.
44. T. Deepa and R. Kumar, "Performance of comparison metrics on M-QAM OFDM systems with high power amplifier," in *World Congress on Information and Communication Technologies* (WICT, 2012), pp. 909–914.

## 1. Introduction

In a dynamic environment of smart cities [1] and networked society with an astonishing number of network subscriptions, growth rate in data traffic and big data, the Internet of Things is challenging the coverage in dense urban areas and indoor environments [2]. To respond to the challenge of high speed and high bandwidth communication networks [3], a new smart lighting technology named visible light communication (VLC) has been developed to relieve the load of existing RF and microwave wireless networks [4] by powering visible photons not only for light generation but also for optical communication. Advantages of VLC over existing wireless systems are network security, worldwide availability, unlicensed spectrum, low power consumption, and the lack of electromagnetic interference among others. Due to these advantages, VLC finds application in a vast range of environments, such as in-building [5], in-hospital [6], in-flight [7], traffic-signaling [8], automotive industry [9, 10], free-space [11], satellite [12], mining [13], and underwater conditions [14,15].

The prosperous development of light-emitting diode (LED)-based solid state lighting technology [16] due to low power consumption, low cost, high luminance efficiency, ease in color rendering, and long lifetime have led to its adoption as common VLC transmitter for providing illumination as well as transmitting data [5,17]. However, LEDs present two serious disadvantages for VLC: first of all, as incoherent light source has an intrinsic limitation in terms of bandwidth modulation around hundreds of MHz due to long spontaneous radiative lifetime [18], and secondly the significant nonlinearities of the output power *versus* input current adversely affects the luminous efficacy [19]. This issue has been circumvented by using highly spectral efficient modulation schemes such as quadrature amplitude modulated orthogonal frequency division multiplexing (QAM OFDM) and discrete multitone modulation (DMT) with pre- and post-equalization circuits [20], power/bit-loading [21] and rate-adaptive [19] algorithm, high-order multiplexing [22], and parallel data transmission [23], thus enabling data rates up to 3 Gbit/s by using either single-phosphor-converted blue LED [24] or red-green-blue (RGB) LEDs triplets [25]. Nevertheless, the low modulation response of LED represents a bottleneck for the future development of ultrahigh-speed VLC systems [26].

As an alternative, high intensity, collimated and monochromatic light from laser diodes (LDs) provides coherent light with much higher modulation bandwidth while maintaining a linear output power with increasing bias current [27]. In this regard, simple approaches using 422-nm LD with non-return-to-zero on-off-keying (NRZ OOK) [28], and 450-nm LD with 64-QAM OFDM [29] modulation techniques have achieved data rates of up to 2.5 Gbit/s, and 9 Gbit/s in free space, respectively. On the other hand, more complex approaches using RGB-LD color mixing have demonstrated high-quality white light [30], high speed data [31], and both high-quality white light with high-speed data [32]. However, single color LD cannot render white light, while RGB-LD color mixing requires complex and costly infrastructures [33]. Therefore, a practical and simple alternative is compulsory to implement real ultrahigh-speed VLC systems with low cost.

A simple strategy using low-cost phosphor-based blue-LD VLC system with QAM OFDM encoding scheme can serve to achieve both high-quality white light and high-speed

#251468 Received 9 Oct 2015; revised 9 Dec 2015; accepted 15 Dec 2015; published 21 Dec 2015

data rate over free space. Additionally, placing phosphor-film at a certain distance from the blue-LD, known as remote phosphor, facilitates thermal management, offering long-term reliability [34]. Moreover, blue-LD light after phosphor conversion results in a scattered beam with the form of diffused bright white light, which is neither collimated nor monochromatic, thus addressing safety concerns for human vision [35].

Furthermore, the VLC capacity can be enhanced by introducing inexpensive optical components within the communication link. For example, linear polarizers enabling new degrees of freedom [36,37], and/or blue filter suppressing slow phosphorescent components [19,20] can serve to augment the limited bandwidth. However, their utility is controversial since they also introduce high signal attenuation [38,39]. Therefore, further studies are needed to confirm the potential of these optical components in LD-based VLC.

In this study, we implement a VLC system based on a 16-QAM OFDM scheme modulating a blue-LD and illuminating a yttrium aluminum garnet (YAG) phosphor-film. The VLC system is optimized by performing a systematic investigation on preparing the phosphor-film, tooling optics-phosphor configurations and adjusting optical components within the VLC link. By changing the phosphor-film composition and optics-phosphor configuration between standalone and mirror-coated, we systematically tune the generated white light from cool day light to neutral light. Furthermore, we achieve a data rate of 4 Gbit/s with a BER of $9.7 \times 10^{-5}$ when using low garnet concentration phosphor-film with mirror-coated configuration in a blue filter-free link due to enhanced blue light transmission in forward direction. The phosphor enables the white-lighting function of the blue-LD based VLC system as a competitive alternative to its counterpart (LED based VLC) for boosting the transmission capability of optical wireless communication.

## 2. Materials and methods

### *2.1 Experimental set-up*

A schematic of the proposed experimental VLC system setup is shown in Fig. 1(a). A single mode fiber-pigtailed 450-nm blue-LD (Thorlabs, LP450-SF-15) is used as the optical source. By mounting the blue-LD onto an LD mount (Thorlabs, LDM9LP), a stable current bias is driven via a benchtop current/TEC controller (Thorlabs, ITC4001). The LD mount provides a SubMiniature version A (SMA) connector to access a bias-tee circuit for RF modulation of the laser's drive current. The RF modulation signal is based on a 16-QAM OFDM signal generated off-line by a homemade MATLAB program in the transmitter (Tx) unit, and uploaded into an AWG (Tektronix, 70001A). The AWG signal is first attenuated 6 dB by an electrical attenuator. Then, the signal is electrically pre-amplified with a 26-dB broadband power amplifier (Picosecond Pulse Labs, 5865, 12 GHz at 3-dB bandwidth) and superimposed to the bias current through the SMA connector to directly modulate the fiber-pigtailed packaged blue-LD. The as-modulated laser beam is collimated by plano-convex lens (Thorlabs, LA1951-A) to irradiate directly a phosphor-film placed at 3 cm distance from the LD. The out-coming white light and blue-LD beam are transmitted through 50 cm free space region, filtered by an optical blue filter (Thorlabs, FB450-10), polarized by a linear polarizer (Thorlabs, DGL10), and focused by a plano-convex lens (Thorlabs, LA1131-A) onto a 12 V biased low noise, high sensitivity silicon APD (Menlo systems, APD210, 1-GHz at 3-dB bandwidth). The APD output is amplified 26 dB by power amplifier. After optical-electrical conversion, the received analog waveform is captured by a DSA (Tektronix, DSA 71604C) with a sampling rate of 100 GSample/s, and decoded offline by a homemade MATLAB program in the receiver (Rx) unit.

#251468 Received 9 Oct 2015; revised 9 Dec 2015; accepted 15 Dec 2015; published 21 Dec 2015

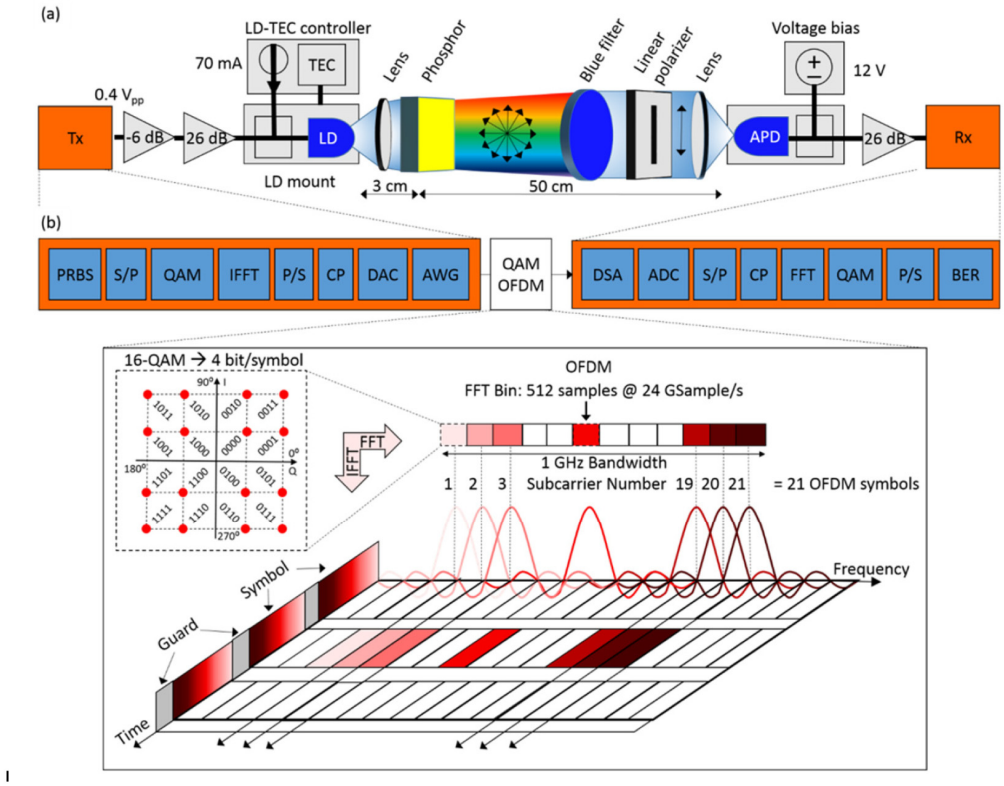


Fig. 1. (a) Experimental set-up configuration of our proposed phosphor-based blue-LD VLC system. (b) Schematic block diagram of the 16-QAM OFDM transmission (Tx) and reception (Rx) units. The inset is the time-frequency scheme of the 16-QAM OFDM data. TEC, thermoelectric cooler; APD, avalanche photodetector; PRBS, pseudo-random binary sequence; S/P, serial-to-parallel multiplexer; P/S, parallel-to-serial demultiplexer; DAC, digital-to-analog converter; ADC, analog-to-digital converter; FFT, fast Fourier transformation; IFFT, inverse fast Fourier transformation; QAM, quadrature amplitude modulation; OFDM, orthogonal frequency-division multiplexing; TS, training symbol; CP, cyclic prefix; FEC, forward error correction; AWG, arbitrary waveform generator; DSA; digital serial analyzer; BER, bit error rate.

### *2.2 RF modulation/demodulation: 16-QAM OFDM implementation*

Figure 1(b) shows the RF modulation/demodulation process of the 16-QAM OFDM signal. High-speed raw data is generated in the Tx unit by a PRBS, divided into parallel binary streams by a S/P multiplexer, encoded with M-QAM levels ($M_{QAM}$ = 16 symbols; $m_{QAM}$ = $\log_2$ 16 = 4 bit/symbol), mapped in an in-phase/quadrature (IQ) constellation diagram, transformed into equally-spaced N-OFDM subcarriers ($N_{OFDM}$ = 21 symbol) with 1 GHz bandwidth ranged from 0.14 to 1.14 GHz by IFFT ($L_{FFT}$ = 512 samples), and converted back into serial data by a P/S demultiplexer. At this point, the data is complemented with 8 additional TS, a CP of 1/32 of the FFT size, and a FEC overhead of 7%. The time-domain signal is converted to a continuous signal by a DAC and loaded into AWG with a sampling rate ($\Delta f$) of 24 GSamples/s. Consequently, a transmission rate ($t_r$) of 4 Gbit/s is calculated as follows:

$$t_r[bit/s] = \frac{\Delta f[sample/s]}{L_{FFT}[sample]} * N_{OFDM}[symbol] * m_{QAM}[bit/symbol] \qquad (1)$$

#251468 Received 9 Oct 2015; revised 9 Dec 2015; accepted 15 Dec 2015; published 21 Dec 2015

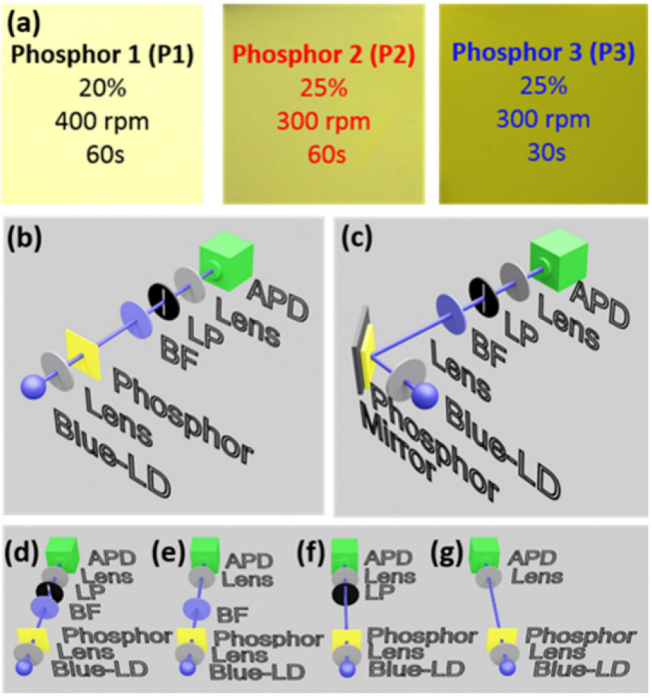


Fig. 2. (a) Photographs of as-synthesized phosphor-film with varying YAG:Ce concentration on PDMS, spin coating speed, and baking time. Experimental setup of our proposed optics-phosphor-films configurations: (b) standalone and (c) mirror-coated. Experimental setups of four different approaches to evaluate the necessity of the optical blue filter (BF) and the linear polarizer (LP): (d) with linear polarizer and with blue filter (LP/BF), (e) without linear polarizer and with blue filter (wLP/BF), (f) with linear polarizer and without blue filter (LP/wBF), and (g) without linear polarizer and without blue filter (wLP/wBF).

Once the waveform is received in the Rx unit, the data is sampled and stored by the DSA. The signal is digitalized by an ADC, synchronized with the training symbol by an auto-correlation algorithm to find the symbol head, divided into parallel data by a S/P multiplexer, filtered of TS and CP, translated and equalized to frequency domain by FFT, de-mapped and decoded into bit streams, converted back to serial to data by P/S demultiplexer, and analyzed to extract the BER performance of each subcarrier and the corresponding constellation map [40].

*2.3 BER and EVM as a standard metric*

We use BER as a standard performance metrics for communication signal quality evaluation since it describes the probability of error in terms of number of erroneous bits per bit transmitted. Under the assumptions of additive white Gaussian noise, data-aided reception and quadratically (L x L) arranged M-QAM constellations, the BER can be estimated from the error vector magnitude (EVM) values, which describes the effective distance of the received complex symbols from their ideal positions in the constellation diagram, according with the following formula [41]:

$$BER \approx \frac{2\left(1-\frac{1}{L}\right)}{\log_2 L} Q\left[\sqrt{\left[\frac{3\log_2 L}{L^2-1}\right]\frac{2}{EVM_{RMS}^2 \log_2 M}}\right] \tag{2}$$

#251468 Received 9 Oct 2015; revised 9 Dec 2015; accepted 15 Dec 2015; published 21 Dec 2015

*2.4 Phosphor-film synthesis, configurations, and approaches*

For yellow phosphor-film, we use cerium-doped yttrium aluminum garnet [$(Y_{1-a}Gd_a)_3(Al_{1-b}Ga_b)_5O_{12}:Ce^{3+}$, abbreviated as YAG:Ce] embedded in poly-dimethylsiloxane (PDMS) matrix [42]. Three phosphor-films P1, P2 and P3 with different color temperature are fabricated by varying the phosphor concentration between 20% and 25% and using different spin-coating parameters as shown in Fig. 2(a). First, micrometer-sized YAG:Ce particles are homogeneously dispersed in a cross-linked PDMS matrix to form the phosphor slurry. In the second step, the phosphor slurry is spin-coated on glass substrate and baked at 70 °C, the parameters for spin-coating/baking time are 400 rpm/60 s, 300 rpm/60 s and 300 rpm/30 s for P1, P2, and P3 respectively. Finally, free-standing phosphor-films are formed by removing them from the glass substrate. The absorption spectra is recorded by UV-670 UV-VIS Spectrophotometer from Jasco.

Two optics-phosphor configurations for each phosphor-film are used to evaluate the white light and the VLC performance: standalone (namely P1, P2, and P3), and mirror-coated (namely M1, M2 and M3) as shown in Fig. 2(b), and 2(c) respectively. The diffused white light emission spectrum and extracted Commission Internationale de l'Éclairage (CIE, 1931) diagram, chromaticity coordinates (x, y), and correlated color temperature (CCT) are recorded with GL Spectics 5.0 Touch Optics spectrometer. Moreover, four different approaches are considered also to evaluate the VLC performance by means of the effectiveness of placing the BF and the LP along the direct line-of-sight (LOS) between blue-LD and APD as shown in Fig. 2(d)-2(g).

## 3. Results and discussions

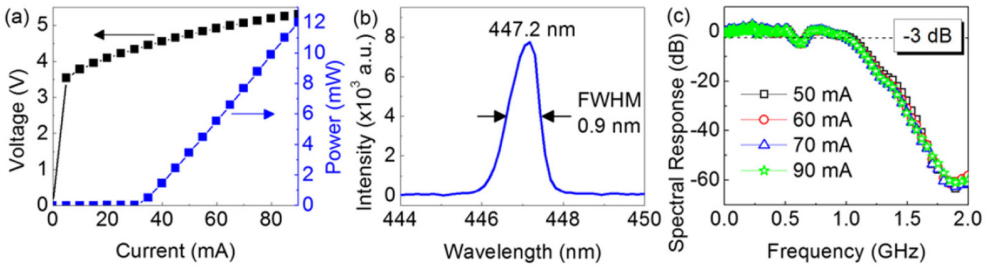


Fig. 3. (a) *L-I-V* curve of the blue-LD under continuous wave operation at 25 °C. (b) Emission spectra of the blue-LD. (c) Small-signal frequency response of the blue-LD in free space with injection currents of 50, 60, 70 and 90 mA.

The light-current-voltage (*L-I-V*) curve of the blue-LD at operation temperature of 25 °C is shown in Fig. 3(a). The threshold current ($I_{th}$) is about 35 mA, and the slope of the *L-I* curve above threshold is 0.27 W/A showing good linearity. However, we considered several factors to accurately modulate the blue-LD signal for optimal VLC operation: (*i*) the LD was driven at $2I_{th}$ (70 mA) to avoid clipping, (*ii*) the peak-to-peak voltage ($V_{pp}$) of the AWG was adjusted to 0.4 $V_{pp}$ to achieve the highest data rate and thus use the full dynamic range of the LD, and (*iii*) a 6 dB attenuator was inserted to eliminate nonlinearities generated from the saturation of the power amplifier. Figure 3(b) shows the blue-LD lasing peak wavelength and full-width at half-maximum (FWHM) are 447.2 nm and 0.9 nm respectively, revealing a blue-narrowband optical carrier for the VLC.

#251468 Received 9 Oct 2015; revised 9 Dec 2015; accepted 15 Dec 2015; published 21 Dec 2015

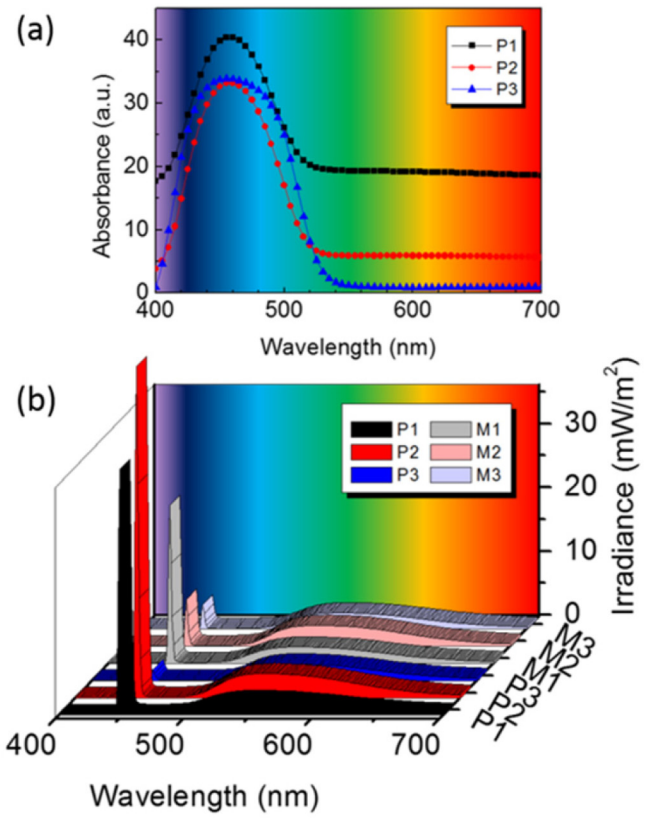


Fig. 4. (a) Absorption spectra of the three phosphor-films P1, P2, and P3 in standalone configuration. (b) Irradiance spectrum of the white light generated by standalone P1, P2, and P3 and mirror-coated M1, M2, and M3 phosphor-films when illuminated by blue-LD under 70 mA and 16-QAM OFDM signal.

Furthermore, to determine the maximum allowable encoding bandwidth of the blue-LD/free-space/APD link, the overall signal frequency response of the system was characterized under different DC bias currents as shown in Fig. 3(c). With increasing bias current, no significant shift in bandwidth is observed, and hence the 3 dB modulation bandwidth is ~1 GHz, which we ascribe to the APD cut-off frequency of 1 GHz. Figure 4(a) shows the absorption spectra of the three YAG:Ce phosphors-films. The three phosphor-films exhibit similar absorbance peak shape within 410 - 510 nm and peak position centered at 450 nm, corresponding to the absorption of $Ce^{3+}$ ions from the 4*f* ground state to the 5*d* excited state. Additionally, Fig. 4(b) shows the spectral irradiance of the generated white light by the phosphor-films with standalone and mirror-coated configurations. The peak wavelengths of the sharp-narrowband blue emissions are fixed for all the cases at 448 nm, corresponding to the blue-LD light transmitted through the phosphor; meanwhile the peak wavelength of the green-yellow broadband (500 - 650 nm) emission is 549 nm for P1 and M1, 551 nm for P2 and M2, and 557 nm for P3 and M3, corresponding to the yellow fluorescence from phosphor. The phosphor absorption in the blue region accounts for $4f \rightarrow 5d$ transition of $Ce^{3+}$ ions while the green-yellow emission results from the Stokes shift caused by the vibration coupling of the excited 5*d*-level. Therefore, the visible irradiance spectra indicates that optical pumping at 448 nm is effective for excitation the green-yellow luminescence broadband from YAG:Ce. However, the absorption of the blue-LD light is more efficient using P1, P2, and M1, which explains the higher intensity at 448 nm. In contrast P3, M2 and M3 have very low

#251468 Received 9 Oct 2015; revised 9 Dec 2015; accepted 15 Dec 2015; published 21 Dec 2015

blue emissions. On the other hand, the green-yellow emission is more intense by using P2 and M2, less intense by using P3, M1, and M3, and weak by using P1.

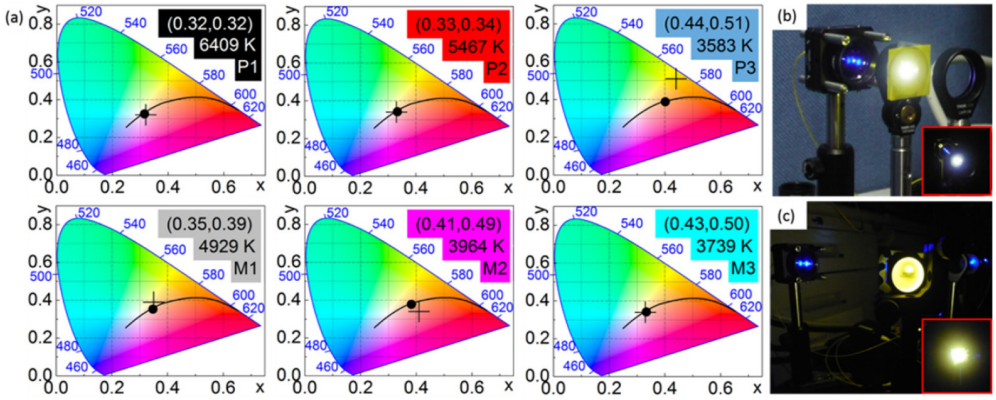


Fig. 5. (a) CIE 1931 chromaticity diagram with lines of constant CCT, (x,y) coordinates from 2° observer, and CCT value obtained from the irradiance spectrum of measured white light generation with phosphor-films in standalone (P1, P2, and P3) and mirror-coated (M1, M2, and M3) configurations. Photographs of the as-generated white light by (b) standalone phosphor-film P1 and (c) mirror-coated phosphor-film M1.

Because blue and yellow are complementary colors, the proper combination of both bands with the correct intensity ratio results in white light generation during transmission. Therefore, we study the color characteristics of the as-generated white light by characterizing the CIE 1931 diagram with chromaticity coordinates (x, y), and CCT of the phosphor-films in standalone (P1, P2 and P3) and mirror-coated (M1, M2 and M3) configurations as it is shown in Fig. 5(a). As a result, P1 with a CCT value of 6409 K is the closest to the 6500 K cool day light, as illustrated in Fig. 5(b). Meanwhile, P3, M2 and M3 occupying a CCT region from 3500 to 4000 K are described as neutral white due to yellower hue of white, see Fig. 5(c). Finally, P2 and M1 with CCT values between 4500 and 5500 K are described as cool white due to their bluish hue. Furthermore, the CIE coordinates (0.32, 0.32) of P1, and (0.33, 0.34) of P2 are the closest to (0.33, 0.33) pure white light, suggesting that the peak intensity of the narrow blue light should be 3 times higher than the broad green-yellow light to render proper white light. Nevertheless, the results demonstrate that CIE chromaticity and CCT of the white light emission is systematically tunable from cool day light to neutral light by adjusting the phosphor-film preparation and/or by using standalone or mirror-coated configurations.

Next, we study the data transmission of 16-QAM OFDM signal within 1 GHz bandwidth from 0.14 to 1.14 GHz in our proposed VLC system. To evaluate the most optimal performance, Fig. 6(a) shows the measured BER for both configurations under four approaches, refer to Fig. 2(d)-2(g). The BER is estimated by the EVM from received constellations (see method section), and is an indicator of free-error transmission as long as the BER is maintained below the 7% pre-FEC threshold of $3.8 \times 10^{-3}$, which is the limit of the conventional FEC algorithm for 16-QAM OFDM, see dashed line in Fig. 6(a) [43, 44]. The results show that the BER monotonically decreases using LP/BF, wLP/BF, LP/wBF, and wLP/wBF approaches. Additionally, in Fig. 6(b)-6(f) we plot the constellations and BER of the most optimum setup (wLP/wBF) for comparison between phosphor-films and optics-phosphor configurations. We observe that P1 and M1 have more condense constellation diagrams and lower BER ($3.2 \times 10^{-5}$, and $2.8 \times 10^{-5}$ respectively) than P2 and M2 ($1.7 \times 10^{-3}$, and $5.3 \times 10^{-4}$ respectively), suggesting that the phosphor-film with 20% garnet concentration has better VLC performance than with 25% garnet concentration. It is also remarkable that M3 has led to a BER as low as $9.7 \times 10^{-5}$ with a condense constellation, when in contrast no data was attainable for P3 due to low signal to noise ratio (SNR).

#251468 Received 9 Oct 2015; revised 9 Dec 2015; accepted 15 Dec 2015; published 21 Dec 2015

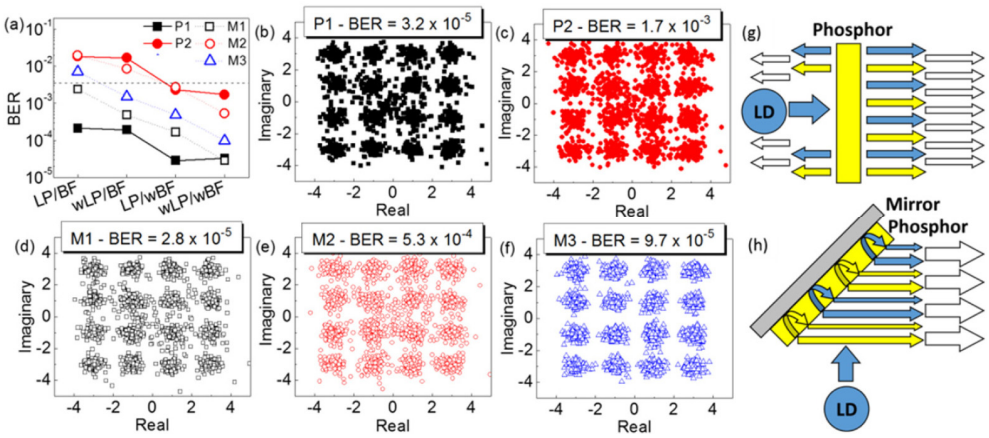


Fig. 6. (a) The measured BER of the transmitted 16-QAM OFDM signal emitted from blue-LD and exciting phosphor-films in standalone P1, and P2, and mirror-coated M1, M2, and M3 configurations under four approaches at receiver side: LP/BF, wLP/BF, LP/wBF, and wPL/wBF. Dashed line indicates the BER of FEC Limit: $3.8 \times 10^{-3}$. Constellation plots and related BER of the transmitted 16-QAM OFDM signal through the wLP/wBF setup approach for phosphor-films in standalone (b) P1, and (c) P2, and mirror-coated (d) M1, (e) M2, and (f) M3 configurations. Schematic of white light generation by blue-LD illumination of phosphor-films in (g) standalone, and (h) mirror-coated configuration.

In fact, phosphor-films with mirror-coated configuration show better VLC performance than with standalone configuration. This can be explained as follows: with standalone configuration, the blue and green-yellow components are reflected and transmitted at the same time, leading to power loss of blue light in transmission direction, see Fig. 6(g). However, with mirror-coated configuration, the reflected light is incorporated back into transmission direction through the reflection within the air gaps between phosphor-film and mirror, thus enhancing the blue light in transmission direction, as depicted in Fig. 6(h).

In addition, the entire measured BER values have shown lower BER values without BF than with BF. In fact, the insertion of BF rejects the slow yellow light component, lowering the received optical power that in turn result in an insertion loss of approximately 3dB, degrading the SNR performance and deteriorating the BER. Therefore, the usage of BF in our proposed VLC system is concluded to be unnecessary as reported elsewhere [38,39]. We also observe that the insertion loss of the LP is negligible for P1 and P2, leading to a BER as good as without LP. Consequently, polarization multiplexing technique with standalone configuration could serve to further boost the data rate [36,37].

## 4. Conclusion

In conclusion, we experimentally validate the feasibility of a 4 Gbit/s VLC system by using a YAG:Ce phosphor-based blue-LD and a 16-QAM OFDM modulation signal. The study evaluates three phosphor-film syntheses combining different garnet concentrations and spin coating factors, two optics-phosphor configurations based on standalone or mirror-coated phosphor-films, and four setup approaches based on the role of a blue filter and a linear polarizer. By adjusting the phosphor-film preparation and optics-phosphor configuration, the generated white light can be systematically tuned from cool day light to neutral light. Nevertheless, pure light results from P1 with CCT value of 6409 K and CIE coordinates of (0.32, 0.32). Additionally, by removing the BF, all the cases under study pass the FEC criteria when transmitting 4 Gbit/s data rate with 16-QAM OFDM signal, since the BF by removing the yellow light component degrades the SNR performance, and thus it is concluded to be unnecessary. However, the best VLC performance with $9.7 \times 10^{-5}$ BER is achieved by using 20% garnet concentration with mirror-coated configuration due to enhanced blue light transmission in forward direction. This demonstration signifies a remarkable ramp toward

#251468 Received 9 Oct 2015; revised 9 Dec 2015; accepted 15 Dec 2015; published 21 Dec 2015

boosting the speed data rate of phosphor-based white light LD for high-performance VLC applications.

**Acknowledgment**

José Ramón Durán Retamal, Hassan Makine Oubei, Bilal Janjua, Tien Khee Ng, Jr-Hau He, Mohamed-Slim Alouini, and Boon S. Ooi gratefully acknowledge the financial support from King Abdullah University of Science and Technology (KAUST), under the baseline funding, and King Abdulaziz City for Science and Technology (KACST) Technology Innovation Center (TIC) for Solid-State Lighting at KAUST. Hassan Makine Oubei, Mohamed-Slim Alouini, and Boon S. Ooi acknowledge funding support from KAUST Competitive Center Funding (Red Sea Research Center). Yu-Chieh Chi, Huai-Yung Wang and Gong-Ru Lin provide the generation and decoding software and process for the QAM-OFDM data format used in the visible light communication experiment. The financial support from the Ministry of Science and Technology, Taiwan under grants MOST 103-2221-E002-042-MY3 and MOST-104-2221-E-002-117-MY3 is acknowledged.

#251468 Received 9 Oct 2015; revised 9 Dec 2015; accepted 15 Dec 2015; published 21 Dec 2015